CrossMark

ORIGINAL PAPER

The Effect of Ag Doping on the Superconducting Properties of $Y_3Ba_5Cu_{8-x}Ag_xO_{18-\delta}$ Ceramics

T. Metin[1] · M. Tepe[1]

Abstract The influence of Ag doping on the microstructural and superconducting properties of $Y_3Ba_5Cu_8O_{18-\delta}$ (Y358) was investigated by means of resistance-temperature (R–T), ac magnetic susceptibility (χ–T), and X-ray diffraction (XRD) measurements. Five different $Y_3Ba_5Cu_{8-x}Ag_xO_{18-\delta}$ (Ag-Y358) bulk ceramic samples were prepared by employing a standard solid-state reaction method with different amounts of Ag doping ($x = 0.0$, 0.1, 0.2, 0.3, 0.4, and 0.5, respectively). The X-ray patterns revealed that all samples corresponded to the orthorhombic $Y_3Ba_5Cu_8O_{18-\delta}$ phase. The transition temperature of Ag-Y358 samples was enhanced from 95 to 97 K with the increase of Ag doping concentration (up to $x = 0.1$). However, when the Ag content exceeded $x = 0.3$ value, the transition temperature of the samples decreased to below 95.6 K. It was found that excess Ag particles filled into the pores of the structure and caused the deterioration of the superconducting properties.

Keywords YBCO superconductor · Ag-doping · Superconducting properties

1 Introduction

Since the discovery of high-temperature superconductors (HTSs) [1], the researchers have conducted intensive studies to improve the performance of superconducting materials

✉ T. Metin
 tuemetin@gmail.com

[1] Faculty of Science, Department of Physics, Ege University, 35100 Bornova, Izmir, Turkey

[2–9]. During these studies, it was recognized that the number of CuO_2 planes and CuO chains in HTS plays an important role in superconducting transition temperature (T_c) and superconducting properties. For example, while Y123 compound has a superconducting transition temperature of 92 K with two CuO_2 symmetrically equivalent planes and one CuO chain, Y124 has only one inequivalent plane and one double chain, with $T_c = 84$ K [10, 11]. Recently, Aliabadi et al. [12] have reported the new Y-based high-temperature superconductor in Y358 that becomes superconducting at 102 K. The Y358 has a crystal structure similar to Y123, though it has five Cu_2O planes and three CuO chains in a per unit cell. According to Tavana and Akhavan [13], to achieve the highest possible transition temperature, one should pump more holes from chains to the oxygen sites of the planes. The substitution at the oxygen site is very important for the formation of superconducting materials. But, in YBCO superconductor systems, the substitution at the rare-earth site or alkaline-earth site would not change the superconducting transition temperature significantly [14–17]. Although it contributes to the development of the electrical and structural properties such as the grain boundaries and weak pinning properties, the partial substitution of rare-earth elements in YBCO superconductor systems does not much have an effect to critical temperature [18–20]. For instance, the substitution studies by heterovalent ions like Ga^{3+}, Al^{3+}, Fe^{3+}, and Co^{3+}, etc. in the CuO basal plane have clearly indicated a noticeable change in the structure without much change in the transition temperature [21].

The partial substitution studies by monovalent Ag ions show that a certain amount of Ag leads to a small increase in the transition temperature; besides, it increases the critical current density and magnetic flux trapping properties [22]. Also, Ag improves the grain size, homogeneity, toughness, etc. [23–25], and provides a better grain orientation,

Fig. 1 XRD patterns of pure and Ag-Y358 ($x = 0.0, 0.1, 0.2, 0.3, 0.4,$ and 0.5, respectively) samples
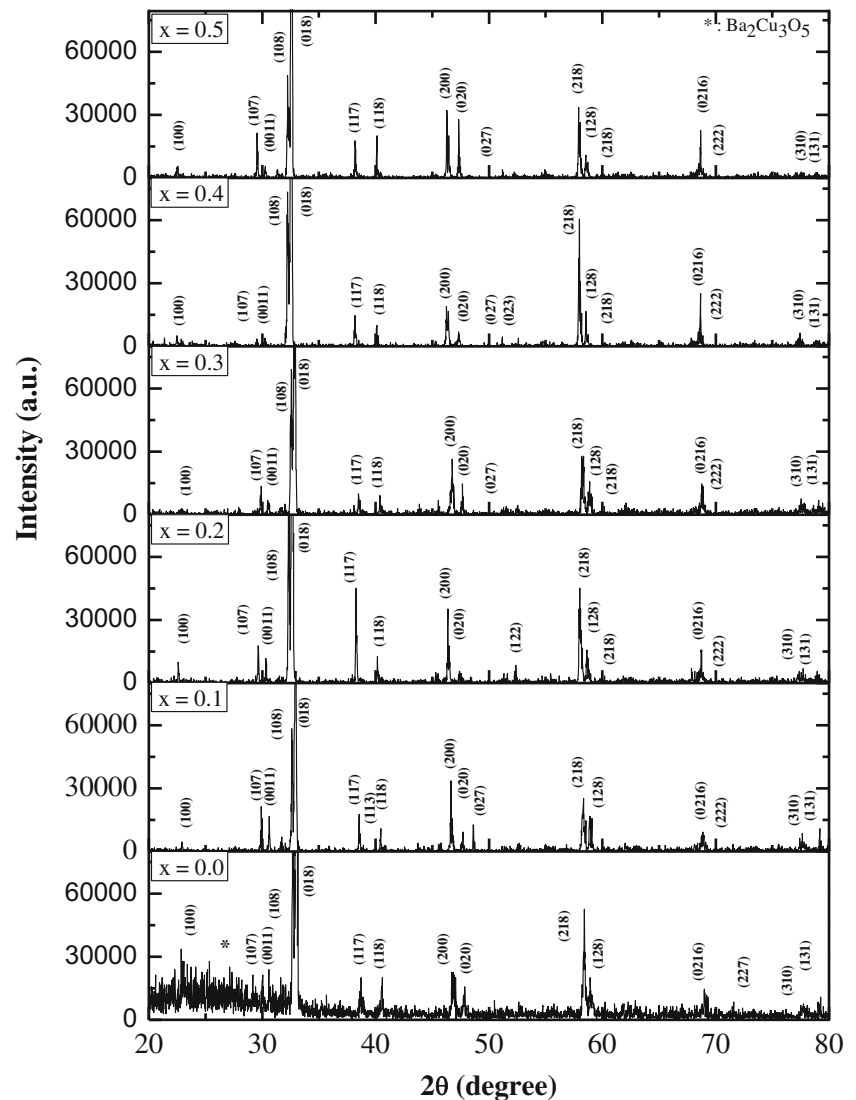
decreasing the electrical resistance in the normal state [26]. However, the excess content of Ag causes an inhibitory factor which increases the grain size [27]. In short, silver plays either a positive or negative role in the improvement of the superconducting properties of Y123 samples changing with Ag doping concentration.
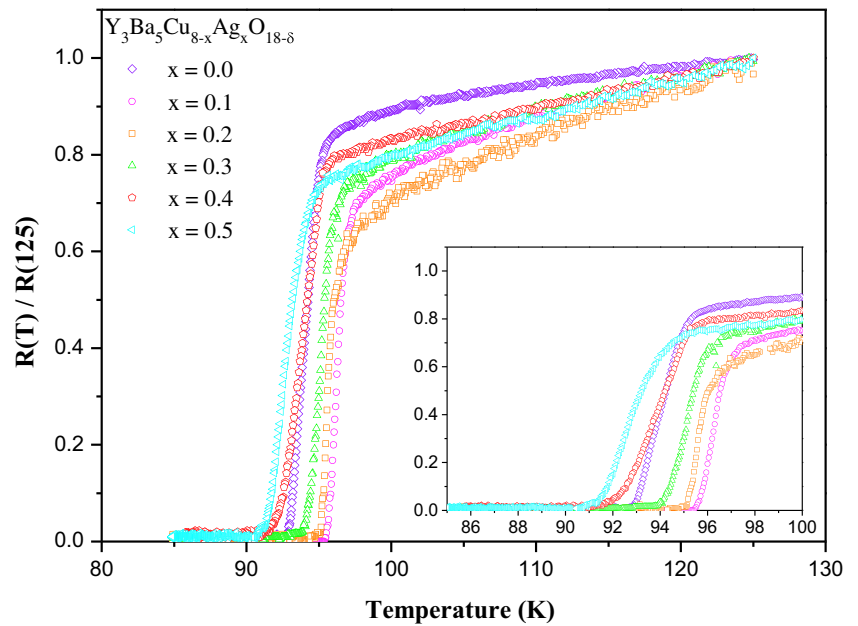
For the preparation process of so far Ag-Y123 materials has been used to various techniques such as electrochemical methods and mixing by adding the metallic Ag or Ag_2O powder to required powders for the pure Y123 material during the solid-state reaction method [28–30]. During the fabrication, Ag atoms can substitute with Cu atoms, which locate at the first CuO plane, in the Y123 grains due to Cu and Ag atoms included in the same group of the periodic table. This causes the microstructural changes in Y123 [31]. But, in some papers, it was reported that Ag does not diffuse into the grains and excess Ag particles fill the pores in the bulk [32].

In this study, we investigated the effect of the superconducting properties and microstructure of Y358 material of the Ag doping on various ratios by creating the ideal

Table 1 The lattice parameters and unit cell volume of pure and Ag-Y358 ($x = 0.1, 0.2, 0.3, 0.4,$ and 0.5) samples

Superconducting sample	Lattice parameters (Å)			Unit cell volume (Å³)
	a	b	c	
$x = 0.0$ (sample A)	3.8951	3.8084	30.8640	457.780
$x = 0.1$ (sample B)	3.8749	3.8040	30.9782	457.111
$x = 0.2$ (sample C)	3.9156	3.8175	30.9782	463.056
$x = 0.3$ (sample D)	3.8749	3.8084	30.7507	453.793
$x = 0.4$ (sample E)	3.8951	3.8370	30.7507	459.584
$x = 0.5$ (sample F)	3.9388	3.8370	30.7507	464.741

Fig. 2 The resistance versus temperature curves of pure and Ag-Y358 ($x = 0.0$, 0.1, 0.2, 0.3, 0.4, and 0.5) samples

2 Experimental Details

Y358 and Ag-Y358 ($Y_3Ba_5Cu_{8-x}Ag_xO_{18-\delta}$) samples were synthesized by the conventional solid-state reaction method. Y_2O_3 (99.99 %), BaO (99.99 %), CuO (99.99 %), and Ag_2O (99.99 %) powders with a stoichiometric ratio of Y:Ba:Cu:Ag = 3:5:8 − x:x ($x = 0.1$, 0.2, 0.3, 0.4, 0.5) were mechanically well mixed and finely grounded for 3 h in an agate mortar. The samples were placed in alumina crucibles and calcined in air at 920 °C for 24 h in a tubular furnace. This calcination process was repeated twice with intermediate grinding. The powders were reground and pressed into pellets of 10 mm diameter and 1 mm thickness under a pressure of 400 MPa. Finally, the pellets were sintered in air at 970 °C for 50 h and then cooled down to room temperature at a rate of 10 °C/min. The samples were named as samples A, B, C, D, E, and F depending on the doping ratios of $x = 0.0$, 0.1, 0.2, 0.3, 0.4, and 0.5, respectively.

X-ray diffraction (XRD) measurements in room temperature were carried out using a Rigaku MultiFlex 2-kW X-ray diffractometer with CuK_α radiation ($\lambda = 1.5418$ Å) in the range $2\theta = 20$–$80°$. The ac electrical measurements were performed using a standard four-probe method on all samples, and contacts were made by using silver paste. For temperature-dependent resistance measurements, the bulk samples were cut into rectangular bars from the pellets using a fret saw and they were thinned by using abrasive paper.

A two-phase SR 530 Lock-in amplifier and a calibrated Lakeshore Pt thermometer were used for the resistance measurements. The ac magnetic susceptibilities of the samples were measured by a mutual inductance bridge method, and also, a two-phase SR 530 Lock-in amplifier was used to pick up in-phase (χ') and out-of-phase (χ'') signals of secondary coils.

3 Results and Discussion

Figure 1 shows the XRD patterns of pure Y358 and Ag-Y358 ($Y_3Ba_5Cu_{8-x}Ag_xO_{18-\delta}$ with $x = 0.1$, 0.2, 0.3, 0.4, and 0.5) samples. The X-ray diffraction patterns in Fig. 1 were compared with some studies in the literature. Also, these studies in the literature were used for the identification of each phase. Based on this information, X-ray diffraction patterns indicate the non-superconducting phase

Table 2 Superconducting transition temperatures of pure and Ag-Y358 ($x = 0.0$, 0.1, 0.2, 0.3, 0.4, and 0.5) samples

Superconducting sample	T_c (on) (K)	T_c (mid) (K)	T_c (off) (K)	ΔT_c (K)
$x = 0.0$ (sample A)	95.6	94.2	93	2.6
$x = 0.1$ (sample B)	97.4	96.3	95.5	1.9
$x = 0.2$ (sample C)	96.5	95.7	95.1	1.4
$x = 0.3$ (sample D)	96.4	95.2	94.1	2.3
$x = 0.4$ (sample E)	95.3	94	91.5	3.8
$x = 0.5$ (sample F)	94.7	93	91.4	3.3

$Ba_2Cu_3O_5$ [33–35]. According to X-ray diffraction patterns, the non-superconducting phase $Ba_2Cu_3O_5$ exists in the crystal structure of pure Y358. The peaks located at 46.83° and 47.70° represent the orthorhombic structure for Ag-Y358. The calculated unit volumes and lattice parameter of each sample are shown in Table 1. The calculated values of parameters a and b for the pure Y358 and Y123 were found to be close to each other, but the value of c parameter for pure Y358 is almost three times of the c parameter for Y123. These results are compatible with the findings reported by Aliabadi et al. [12]. When the calculated lattice parameters for all samples were carefully analyzed, it was found that there was a little deviation from an orthorhombic cell. The change in the values of all lattice parameters (a, b, and c) can represent that Cu atoms may be substituted by Ag atoms. The obtained lattice parameters are in agreement with other studies [36–38]. As seen in sample C, the increase in the volume of the unit cell with Ag doping clearly indicates that Ag goes to the lattice sites in the grains.

Figure 2 shows the change in electrical resistance versus temperature for pure and Ag-Y358 samples near the superconducting transition. It can be seen from these curves that the transition temperatures slightly changed by the increase of Ag content. This is an evidence of much better links between the superconducting grains. Table 2 shows the transition temperature of pure and $Y_3Ba_5Cu_{8-x}Ag_xO_{18-\delta}$ with $x = 0.0, 0.1, 0.2, 0.3, 0.4,$ and 0.5. The transition temperature of B sample reached to 97.4 K with the increase of Ag concentration for $x = 0.1$. This slight increase in T_c may be depending on the optimization of hole density and changes in the lattice vibration of Y123 due to the substitution of Cu

ions by heavier Ag ions. For E and F samples, $T_{c,zero}$ was decreased down to values below the $T_{c,zero}$ of the pure Y358. Although the critical temperature of B samples is higher than that of C samples, the superconducting phase transition curve of C sample is sharper. Pure and Ag-Y358 samples exhibit a metallic behavior in the normal phase. Consequently, the normal resistance of samples decreases linearly by the concentration of silver increasing up to $x = 0.2$. The reason of the reduction in resistance of the samples in the normal state may be related with the decrease occurring in the resistance of grain boundary due to Ag atoms with low concentration which resides between the grains.

The ac magnetic susceptibilities of the samples were measured with a frequency of 1 kHz in the temperature range 77–100 K, and Fig. 3 shows that the temperature variation of both real (χ') and imaginary (χ'') components of diamagnetic signal highly depends on Ag concentration. The change of χ' versus T for each of the sample has a distinct two-stage fall-off. This two-stage fall-off gives the information about inter- and intragranular superconductivity [39]. The first stage is the range between T_c and the starting point of the second-stage fall-off at the lower temperature than T_c. The second stage is related with a measure of the magnetic shielding of applied field B by the intergrain supercurrent passing from weak links. The peak formation of χ'' originates from hysteresis loss arising due to the penetration of magnetic flux in the intergranular network of weak links [40].

Figure 3 shows that not only the first and second fall-offs of χ' but also the peak position of χ'' strongly depend on Ag doping. This is an indicator that Ag atoms are substituted by Cu atoms at lattice sites in grains. The results of

Fig. 3 The ac magnetic susceptibility-temperature curves of pure and Ag-Y358 ($x = 0.0, 0.1, 0.2, 0.3, 0.4,$ and 0.5) samples
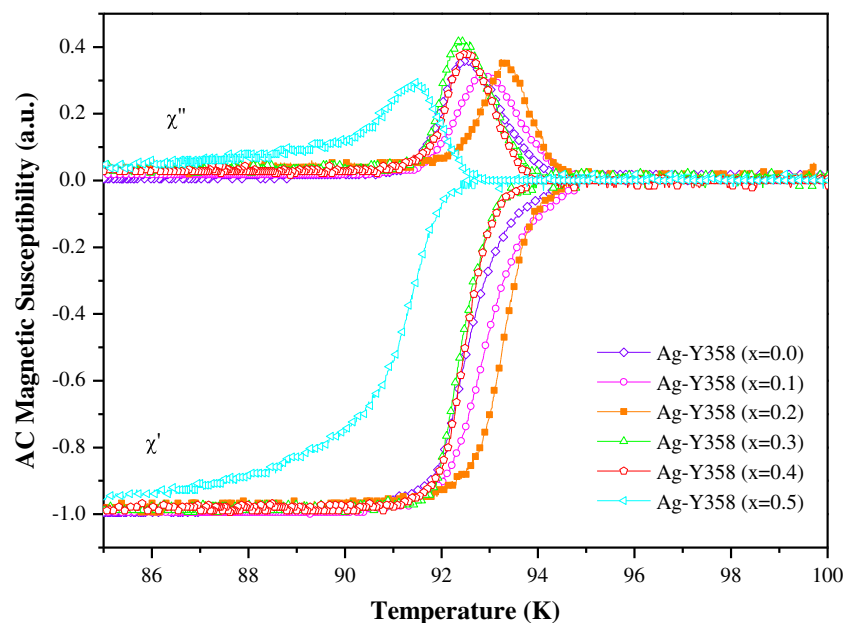
ac magnetic susceptibility for samples C, D, E, and F show that diamagnetic transition temperatures shifted to the low values. Sample A (pure) showed the superconducting transition at $T_c = 94.6$ K. Although the diamagnetic transition temperature of sample B ($x = 0.1$) reached to $T_c = 95$ K, the strongest diamagnetic behavior was observed for the C samples ($x = 0.2$) at $T_c = 94.7$ K. Sample C has a very homogenous Y358 phase due to very sharp diamagnetic transition at 94.7 K. As seen from Fig. 3, the diamagnetic transition temperatures of D, E, and F samples decrease from $T_c = 94$ K down to 93 K. It seems the excess Ag in the case of D, E, and F samples causes a degradation of the superconducting properties of grain boundaries and their alignments. The changes of ac magnetic susceptibility depending on temperature indicate that the limited amount of silver doping develops the transition temperature and diamagnetic behavior of Y358 ceramics while the excess amount of the Ag causes the degradation of these properties.

4 Conclusion

In this study, we investigated the effect of Ag doping on the superconducting and electrical transport properties of Y358 system. In the certain concentration of Ag values (up to $x = 0.2$), an improvement in the microstructure and diamagnetic transition temperature of the samples was observed. The smaller Ag dopants improve the intergranular network of weak links, grain sizes, and their orientations. The porosity of Ag-Y358 significantly decreases because the Ag particles fill the pores, thus, as a consequence, increasing the effective density of Ag-Y358 samples. However, the higher amount of silver plays a preventive role in the growth of the grains of Y358. This shows lower performance for the high current applications. The results obtained are similar with those in the literature about the Ag-doped YBCO.

References

1. Bednorz, J.G., Muller, K.A.: Z. Phys. B **64**, 189–193 (1986)
2. Maeda, H., Tanaka, Y., Fukutomi, M., Asano, T.: Jpn. J. Appl. Phys. **27**, 209–210 (1988)
3. Mukarami, M., Sakai, N., Higuchi, T., Yoo, S.I.: Supercond. Sci. Technol. **9**, 1015–1032 (1996)
4. Chen, D.X., Pardo, E., Sanchez, A., Bartolome, E.: Appl. Phys. Lett. **89**, 072501 (2006)
5. Hanic, F., Cigan, A., Burchta, S., Manka, J., Zrubec, V.: Meas. Sci. Rev. **1**, 1 (2001)
6. Foerster, C.E., Lima, E., Rodrigues Jr. P., Serbana, F.C., Lepienski, C.H., Cantao, M.P., Jureo, A.R., Obradors, X.: Braz. J. Phys. **38**, 3A (2008)
7. Parthasarathy, R.: Int. J. Adv. Appl. Phys. Res., 6–12 (2016)
8. Nishiura, H., Suzuki, R.O., Ono, K.: J. Am. Ceram. Soc. **81**, 2181–87 (1998)
9. Wada, T., Adachi, S., Mihara, T., Inaba, R.: Jpn. J. Appl. Phys. **26**(5), 706–708 (1987)
10. Wu, M.K., Ashburn, J.R., Torng, C.J., Hor, P.H., Meng, R.L., Gao, L., Huang, Z.J., Wang, Y.Q., Chu, C.W.: Phys. Rev. Lett. **58**, 908–910 (1987)
11. Marsh, P., Fleming, R.M., Mandich, M.L., Desantolo, A.M., Kwo, J., Hong, M., Martinez-Miranda, L.J.: Nature **334**, 66 (1988)
12. Aliabadi, A., Farshchi, Y.A., Akhavan, M.: Physica C. **162**, 281–284 (2009)
13. Tavana, A., Akhavan, M.: Eur. Phys. J. B **73**, 79–83 (2010)
14. Skakle, J.M.S.: Mat. Sci. Eng. **R23**, 1–40 (1998)
15. Takarama-Muromuchi, E., Uchida, Y., Kato, K.: Jpn. J. Appl. Phys. **26**(12), 2087–2090 (1987)
16. Hor, P.H., Meng, R.L., Wang, Y.Q., Gao, L., Huang, J., Bechtold, J., Forster, K., Chu, C.W.: Phys. Rev. **58**(18), 1891–94 (1987)
17. Veal, B.W., You, H., Paulikas, A.P., Shi, H., Fang, Y., Downey, J.W.: Phys. Rev. B **42**(7), 4770–73 (1990)
18. Sungwong, P., Higgins, J.S., Tsui, Y., Raine, M.J., Hampshire, D.P.: Supercond. Sci. Technol. **26**(10 pp), 095006 (2013)
19. Salamati, H., Kameli, P.: Solid State. Commun. **125**, 407 (2003)
20. Mendoza, E., Puig, T., Varesi, E., Carrillo, A.E., Plain, J., Obradors, X.: Physica C **334**, 7–14 (2000)
21. Salamati, H., Babaei-Brojeny, A.A., Safa, M.: Supercond. Sci. Technol. **14**, 816–819 (2001)
22. Rani, P., Jha, R., Awana, V.P.S.: J. Supercond. Nov. Mag. **26**, 2347–2352 (2013)
23. Tepe, M., Avci, I., Kocoglu, H., Abukay, D.: Solid State Commun. **131**, 319–323 (2004)
24. Diko, P., Fuchs, G., Krabbes, G.: Physica C **363**, 60 (2001)
25. Kohayashi, S., Yoshizawa, S., Miyairi, H., Nakane, H., Nagaya, S.: Mat. Sci. Eng. **B53**, 70–74 (1998)
26. Miller, J.H., Holder, S.L., Hunn, J.D., Holder, G.N.: Appl. Phys. Lett. **54**, 2256 (1989)
27. Diko, P., Krabbes, G., Wende, C.: Supercond. Sci. Technol. **14**, 486–495 (2001)
28. Petrisor, T., Giurgiu, A., Ciontea, L.: Appl. Supercond. **1**, 1219 (1993)
29. Robers, B., Carmona, F., Flandroiss, S.: Physica C **204**, 71 (1992)
30. Matsumoto, Y., Koinuma, M., Yamamoto, H., Nishimori, T.: Solid State Ionics **95**, 309–314 (1997)
31. Taylor, C.R., Greaves, C.: Physica C **235**, 40853 (1994)
32. Nguyen-van-Huong, C., Crampin, E., Laval, J.Y., Dubon, A.: Supercond. Sci. Technol. **10**, 85–94 (1997)
33. Srinivasan, K.C., George, T., Padaikathan, P.: J. Minerals & Charact. & Eng. **10**, 1277–1283 (2011)
34. Gholipour, S., Daadmehr, V., Rezakhani, A.T., Khosroabadi, H., Tehrani, S.F., Akbarnejad, H.R.: J. Supercond. Nov. Magn. **25**, 2253–2258 (2012)
35. Akduran, N.: J. Low Temp. Phys. **168**, 323–333 (2012)
36. De Azambuja, P., Junior, P.R., Jurelo, A.R., Serbena, F.C., Foerster, C.E., Costa, R.M., de Souza, G.B., Lepienski, C.M., Chinelatto, A.L.: Braz. J. Phys. **39**(4), 638–644 (2008)
37. Gangopadhyay, A.K., Mason, T.O.: Physica C **178**, 64 (1991)
38. Jon, J., Singh, J.P., Poeppel, R.B., Gangopadhyay, A.K., Mason, T.O.: J. Appl. Phys. **71**, 2351 (1992)
39. Yamamoto, K., Mazaki, H., Yausoka, H., Katsuyama, S., Kosuge, K.: Phys. Rev. B **46**(2), 1122–1129 (1991)
40. Behera, D., Mishra, N.C., Patnaik, K.: J. Supercond. **10**, 1 (1997)